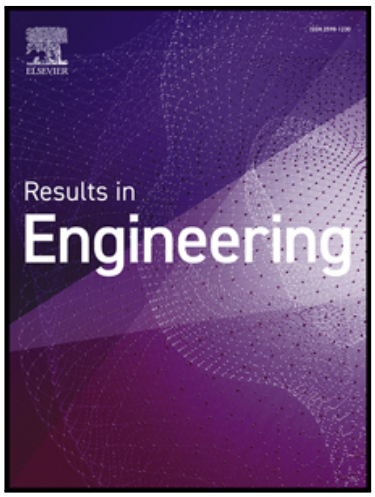

Vacuum pyrolysis of olive pomace for biochar production: Enhancing carbon stability and soil nutrient supply

Walid Chmingui , Imene Dridi , Hanen Zaier , Thomas Z Lerch , Claude Hammecker , Mohamed Hachicha

PII: S2590-1230(25)04706-1
DOI: https://doi.org/10.1016/j.rineng.2025.108662
Reference: RINENG 108662

To appear in: *Results in Engineering*

Received date: 1 September 2025
Revised date: 19 November 2025
Accepted date: 8 December 2025

Please cite this article as: Walid Chmingui , Imene Dridi , Hanen Zaier , Thomas Z Lerch , Claude Hammecker , Mohamed Hachicha , Vacuum pyrolysis of olive pomace for biochar production: Enhancing carbon stability and soil nutrient supply, *Results in Engineering* (2025), doi: https://doi.org/10.1016/j.rineng.2025.108662

Highlights

- First application of vacuum pyrolysis to olive pomace for biochar production.
- Vacuum pyrolysis achieved 30.9 wt.% yield and enhanced carbon retention by ~20 %.
- Biochar showed high stability (H/C = 0.03; O/C = 0.18) and strong aromaticity for long-term sequestration.
- Produced biochar was nutrient-rich (K, P, Ca) with high CEC (56.2 cmolc kg^{-1}), suitable for soil improvement.
- Process reduced inert-gas demand and generated energy-rich syngas, supporting circular-bioeconomy systems.

Vacuum pyrolysis of olive pomace for biochar production: Enhancing carbon stability and soil nutrient supply

Author names

Walid Chmingui,[a,b,*], Imene Dridi [b], Hanen Zaier [c], Thomas Z Lerch [d], Claude Hammecker [e], Mohamed Hachicha [a]

ORCID IDs

Walid Chmingui: https://orcid.org/0000-0002-2449-926X

Thomas Z Lerch: https://orcid.org/0000-0003-3984-1643

Claude Hammecker: https://orcid.org/0000-0001-5594-4891

Affiliations

a *Laboratory of Non-Conventional Water Valorization, National Research Institute for Rural Engineering, Water, and Forestry (INRGREF), University of Carthage. P.O. Box 10. Hedy Karray Street, 2080, Ariana, Tunisia*

b *Laboratory of Sedimentary Basins and Petroleum Geology, Department of Geology, Faculty of Sciences of Tunis, University of Tunis El Manar, Tunis. 2092 El Manar Tunis, Tunisia*

c *Laboratory of Integrated Olive Production, Olive Tree Institute, Hedi Karray Street, P.O. Box 208, 2080, Ariana, Tunisia*

d *Institute of Ecology and Environmental Sciences of Paris, UMR 7618 (CNRS, SU, IRD, UPEC, INRAE, UPC), 93140 Bondy, France*

e *Soil-Agrosystem-Hydrosystem Interaction Lab-LISAH, Place Pierre Viala, 2, 34060, Montpellier, France*

Corresponding author

*Walid Chmingui: walid.chmingui@ingref.ucar.tn

Abstract

Olive pomace (OP), a significant agro-industrial byproduct in Mediterranean countries, poses considerable disposal challenges and offers potential as a feedstock for engineered biochar production. Conventional pyrolysis of OP has been widely studied and often yields biochar with limited aromaticity and variable nutrient content. However, no prior work has explored the potential of vacuum pyrolysis for this residue. Addressing this research gap, this study investigates the use of vacuum pyrolysis (500°C, 15–20 kPa, 2 h) to transform OP into a stable and nutrient-rich biochar. The process yielded 30.9 wt.% biochar with 68.7% fixed carbon, representing an improvement of 20% in carbon retention compared with atmospheric pyrolysis. Elemental ratios (H/C = 0.03 and O/C = 0.18) confirmed high aromaticity and long-term stability, while mineral enrichment underscored high agronomic value. The biochar displayed a cation exchange capacity of 56.2 cmolc/kg and 79% porosity, properties favorable for nutrient cycling, and soil remediation. The carbon sequestration potential was estimated at 2.6 tCO_2eq per ton of biochar applied and heavy metals were below international thresholds, ensuring environmental safety. Beyond material characterization, the work highlights engineering advantages, including reduced inert gas requirements and a reusable syngas fraction (64.6 wt.%) that can offset energy costs. However, as the study was conducted at a single pressure level, the specific contribution of vacuum conditions requires further confirmation through multi-pressure trials. Such results position vacuum pyrolysis as a promising technology for waste valorization, carbon management, and climate-smart agriculture, while future research should address field validation, contaminant screening, and life-cycle performance.

Keywords: Olive pomace; Vacuum pyrolysis; Biochar engineering; Carbon sequestration; Nutrient enrichment

1. Introduction

The increasing accumulation of agro-industrial waste poses significant environmental and management challenges, particularly in regions where agricultural activities are extensive (Yaashikaa et al., 2020). Among these residues, olive pomace (OP), a byproduct of olive oil production, is generated in large quantities across Mediterranean countries (El-Bassi et al., 2021; Marks et al., 2020). Spain, the world's leading olive oil producer, generates several million tons of olive pomace annually (4.0 million tons in 2022), with comparable quantity in Tunisia, Italy, and other olive-producing countries (P. Rueda et al., 2022). Globally, the olive oil sector produces more than 30 million tons of byproducts each year, 40–50% of which is solid pomace with 60–70% moisture content (Afshar & Mofatteh, 2024; Vandana et al., 2025). The inappropriate disposal of OP contributes to greenhouse gas emissions and environmental pollution due to its acidity, high phenol content, and other organic compounds (Anvari et al., 2024; Enaime et al., 2024). However, it is considered a suitable feedstock for thermochemical valorization since it is rich in cellulose, hemicellulose, lignin, and residual oils (Miranda et al., 2008; Rambhatla et al., 2025). Typically, olive pomace contains 25–35 wt.% lignin, 20–25 wt.% cellulose, and 15–20 wt.% hemicellulose, providing an energy content of 17–19 MJ kg^{-1} (Subbiah et al., 2025)

Biochar production via pyrolysis has emerged as a promising pathway to transform biomass wastes into carbon-rich materials with multiple environmental and agronomic benefits. When applied to soil, biochar can significantly improve physical properties and porosity, modulate pH, enhance nutrient content and cation exchange capacity, while simultaneously mitigating greenhouse gas emissions, and contribute to long-term carbon sequestration (Agbede & Oyewumi, 2022; Hossain et al., 2020). Global life-cycle assessments estimate that large-scale

biochar deployment could sequester 66 to 130 billion metric tons of CO_2 eq century^{-1} (Afshar & Mofatteh, 2024).

Recent reviews confirm its potential role in soil fertility and pollutant remediation (Enebe et al., 2025; Munzeiwa et al., 2025). However, its physicochemical properties such as porosity, aromaticity, pH, and elemental composition are influenced by feedstock characteristics and pyrolysis conditions, which dictate carbon stability, aromaticity, and nutrient retention (Ippolito et al., 2020; Ravindiran et al., 2024). Optimizing these properties is crucial for adapting biochar to specific applications in agriculture, environmental remediation, or energy production (Martínez-Toledo et al., 2025).

Conventional slow pyrolysis of olive pomace (fixed-bed or N_2-purged reactors under atmospheric pressure) has been extensively studied. It often presents trade-offs between biochar stability and nutrient enrichment, depending on the feedstock composition and reactor configuration. For instance, Aissaoui et al. (2023) reported that the mineral composition of OP biochar produced at 600 °C with a residence time of 15 min was particularly rich in K, Ca, and P (8.70, 8.73, and 0.67 mg g^{-1}, respectively). In contrast, Azzaz et al. (2022) observed markedly lower concentrations (3.10, 1.39, and 0.16 mg g^{-1}) for biochar obtained at the same temperature but with a longer residence time of 60 min. Such variability illustrates how process conditions govern nutrient retention. While higher pyrolysis temperatures enhance carbon aromaticity and long-term stability, they simultaneously promote volatilization of alkali and alkaline-earth elements, thereby reducing agronomic value (Lustosa Filho et al., 2024). Conversely, lower-temperature operations tend to preserve mineral nutrients but yield less-stable biochars (Kavdır et al., 2023). These opposing effects constrain the dual objective of maximizing both agronomic and climate-mitigation benefits from OP-derived biochars.

Vacuum pyrolysis, which operates under low-pressure and oxygen-free conditions, offers distinct advantages and presents a promising alternative (Ruan et al., 2018). By minimizing secondary reactions, vacuum pyrolysis enhances the retention of fixed carbon and inorganic nutrients, reduces volatile losses, and improves structural stability (Divyangkumar et al., 2024; Roy et al., 2005; Sharma et al., 2024). Compared to conventional methods such as hydrothermal carbonization, torrefaction, or traditional pyrolysis, vacuum pyrolysis required reduced energy for heating inert gases and condensation processes. In conventional systems, inert gases like nitrogen and argon are typically used to displace oxygen and prevent combustion. However, vacuum pyrolysis achieves an oxygen-free environment by simply reducing system pressure, thereby eliminating the energy demand associated with preheating inert gases. Furthermore, energy efficiency analyses report up to 25% reduction in auxiliary gas consumption and 10–15% increase in net energy recovery under vacuum operation (Subbiah et al., 2025). Reduced pressure significantly influences both the yield and quality of pyrolysis products (Roy et al., 2005). Vacuum pyrolysis has been tested with several lignocellulosic feedstocks like rice husk, peanut shells, and almond shells. It has been shown to minimize re-condensation reactions and enhances biochar stability and nutrient retention (Divyangkumar et al., 2024; Sharma et al., 2024; Uras-Postma et al., 2014). Despite these advantages, the application of vacuum pyrolysis to OP remains unexplored and has not been reported in the existing literature. This represents a critical research gap, as the process could potentially mitigate the limitations of conventional OP biochar. This study contributes in filling this gap and aims to fill a key knowledge gap in biochar engineering for Mediterranean land use contexts within climate-smart agriculture and circular bio-economy goals by valorizing abundant agricultural wastes potentially harmful for the environment. Therefore, the specific objectives of this study were to:

- Produce biochar from olive pomace using vacuum pyrolysis for the first time.
- Comprehensively characterize the physicochemical, structural, and thermal properties of the resulting biochar.
- Evaluate its suitability for soil application based on international biochar standards (IBI, EBC), focusing on carbon stability, nutrient content, and environmental safety.
- Assess the engineering advantages of the vacuum pyrolysis process for this specific feedstock.

2. Material and Methods

2.1. Feedstock collection and preparation

Fresh olive pomace (OP) was collected from a three-phase olive oil extraction mill in Ariana, Tunisia (36.8592° N, 10.0061° E), adhering to local environmental regulations to prevent untreated residue discharge. The material consisted of pulp, stone fragments, and residual oil, characterized by high water content (50-60%). It was air-dried and then oven-dried to constant weight at 60 °C, homogenized, sieved (<2 mm), and stored at room temperature in airtight containers prior to pyrolysis. Proximate and ultimate analyses of OP were conducted to establish baseline composition.

2.2. Vacuum pyrolysis setup and operating conditions

Pyrolysis experiments were conducted in a laboratory-scale reactor (capacity: 3 kg) at the National Institute of Rural Engineering, Water, and Forests (INRGREF, Tunisia) using a custom-built vacuum pyrolysis unit (Figure 1). The system comprised a muffle furnace, an airtight reaction chamber connected to a vacuum pump (operating at 15–20 kPa), a temperature controller, a condensation assembly for bio-oil collection and a gas-collection cylinder. Prior to experimental runs, the vacuum pyrolysis system underwent rigorous

calibration and performance verification. To assess process reproducibility, ten independent pyrolysis runs were performed using feedstock from the same homogenized batch.

The feedstock was subjected to thermal treatment at 500 ± 3°C for 2 h with a heating rate of 25°C min^{-1} and a pressure of 15 ± 1 kPa, processing approximately 3 kg of dried OP per run. The selected conditions (500°C, 15–20 kPa) represent optimized parameters based on preliminary trials and literature guidance for maximizing both carbon retention and energy efficiency (Sharma et al., 2024; Uras-Postma et al., 2014). Future investigations could explore a broader parameter space to further optimize biochar yield, fixed carbon, and nutrient retention. After pyrolysis, biochar samples were cooled under inert conditions, stored in airtight containers, and analyzed within 30 days to prevent moisture uptake and contamination.

Product yields for biochar, bio-oil, and syngas were calculated on a dry weight basis using the following equations:

$$\text{Biochar (\%)} = (\text{mass of biochar} / \text{mass of feedstock}) \times 100 \quad \textbf{(1)}$$

$$\text{Bio-oil (\%)} = (\text{mass of oil} / \text{mass of feedstock}) \times 100 \quad \textbf{(2)}$$

$$\text{Syngas (\%)} = 100 - (\text{biochar \%} + \text{bio-oil \%}) \quad \textbf{(3)}$$

2.3. Proximate and ultimate analyses

Proximate analysis (moisture, volatile matter, ash, fixed carbon) was determined following ASTM D1762-84. Energy metrics, including the higher heating value (HHV), the energy densification (Ed), the fuel ratio (Fr), and the thermal stability (Ts) indexes, were calculated from empirical relationships following Weber and Quicker (2018). Elemental composition (C, H, N, S) of OP and biochar was determined using a CHNS analyzer (CHNS-O analyzer, Flash 2000, Thermo Scientific, USA). Oxygen content was calculated by difference. Atomic ratios

(H/C, O/C) were derived to assess carbon stability and aromaticity, according to IBI and EBC guidelines. The results were reported as mean ± SD after all analyses were performed in triplicate or more.

2.4. Thermal and stability assessments

Thermal stability and carbon fractions were determined by Rock-Eval 6 (Vinci Technologies, France). Total organic carbon (TOC), hydrogen index (HI), oxygen index (OI), and Tmax were measured (n=4) to evaluate recalcitrance and classify carbon domains.

Thermogravimetric and derivative thermogravimetric (DTG) analyses (n=3) were performed on a DSC-TGA (SDT Q600, TA Instruments) under nitrogen flow (60 mL min^{-1}). Samples (14 mg) were heated from 25 to 1000°C at 10°C min^{-1}. Mass loss stages were interpreted in relation to devolatilization and carbonization processes, following approaches in Singh et al. (2020) and Chaturvedi et al. (2023).

2.5. Physicochemical characterization

The pH and electrical conductivity (EC) were measured in water suspensions (1:2.5 and 1:5 w/v, respectively). The tapped method was used to measure bulk density (ASTM, 2018), and particle density by water pycnometer (ASTM, 2014). While total porosity (%) was calculated from bulk and particles density. All analyses were done in triplicate and the results were reported as means ± SD.

2.6. Mineral composition and nutrient analysis

Major and trace elements in ashes derived from OP biochar were quantified by inductively coupled plasma–optical emission spectroscopy (ICP-OES, PerkinElmer, Optima 8000) after acid digestion (HNO_3/HCl, 3:1). Cation exchange capacity (CEC) was determined using the ammonium acetate method at pH 7. While exchangeable phosphorus was extracted using 0.5 M $NaHCO_3$ at pH 8.5.

2.7. Structural and morphological analysis

Biochar and OP samples were analyzed using FTIR (Bruker Tensor 27, MA, USA) in the range 4000–400 cm^{-1} to identify functional groups. Crystalline phases were identified using an X-ray diffractometer (PANalytical X'Pert PRO, CuKα, 40 kV, 30 mA). Diffractograms were scanned from 5°–80° (2θ). Morphological features were examined using scanning electron microscopy (ZEISS EVO LS15, Germany) at 15 kV. Biochar porosity and surface features were documented at magnifications up to 3000×.

2.8. Environmental impacts assessment

To evaluate the environmental performance of vacuum biochar, three indicators were considered: (i) stable sequestered carbon, (ii) greenhouse gas emission avoidance, and (iii) environmental safety.

(i) The mass yield of biochar (Y, wt.%) and its carbon content (C, wt.%) were used to estimate the amount of stable carbon sequestered per ton of olive pomace, following the IPCC Tier 1 methodology (IPCC, 2019):

$$C_{sequestered} = (Y \times C \times f_{stability}) / 100 \quad \textbf{(4)}$$

where $f_{stability}$ is the fraction of carbon considered resistant to mineralization. A conservative stabilization efficiency of 70% was applied, consistent with IBI and EBC guidelines. The result was expressed as CO_2 equivalents using a conversion factor of 44/12.

(ii) The avoided emissions and fertilizer-equivalent benefit were estimated, following the GHG inventory method described in Woolf et al. (2021). The baseline emissions (0.4–0.7 tCO_2eq per ton), for unmanaged olive pomace, was derived from literature (Goktepeli et al., 2024).

(iii) ICP data were used to check compliance with heavy metal thresholds of the European Biochar Certificate (EBC). While polycyclic aromatic hydrocarbons (PAHs) were not directly measured, but risks were qualitatively assessed based on process conditions.

2.9. Statistical analysis

All analyses were performed in triplicate or more and the results are expressed as mean ± standard deviation. Confidence intervals (95 %) were calculated for key variables (yield, fixed carbon, elemental composition) to quantify analytical uncertainty. Variability across replicates remained below 5 %, confirming experimental reproducibility and robustness of the reported trends. Analytical accuracy was validated using certified reference materials for elemental analysis and Figures were generated with Matplotlib graphical Python library and Microsoft Excel.

3. Results and discussion

3.1. Pyrolysis product yields distribution

Vacuum pyrolysis of olive pomace at 500°C under 15–20 kPa produced three fractions: biochar, condensable liquids, and non-condensable gases. The pyrolytic product distribution, showed increased biochar yield and reduced bio-oil output under vacuum conditions. In the context of olive pomace, recent reviews suggest that pyrolysis can produce biochar yields ranging from approximately 25–35%, while bio-oil yields are typically in the range of 30% to 45%, with the remaining mass converted into gases such as CO, H_2, and CH_4. These figures are consistent with the general trends observed in biomass pyrolysis literature, where higher temperatures tend to favor gas production over biochar and bio-oil, whereas lower temperatures favor bio-oil and biochar formation (İlay, 2020).

The solid yield exceeded values obtained by conventional slow pyrolysis, at similar temperatures (Table 1). This difference is attributed to the vacuum environment, which reduces secondary cracking and improves carbon retention in the solid phase. Consequently, more carbon is retained within the biochar matrix, increasing the solid yield (Alazzaz et al., 2020; Vilas-Boas et al., 2024).

Table 1. Distribution of pyrolysis products from vacuum and conventional processes applied to olive pomace at 500°C.

Product	This study (Vacuum pyrolysis) (wt.%)	Conventional pyrolysis (wt.%)	Interpretation
Biochar	30.9 ± 1.2	20–27	Higher solid yield under vacuum
Bio-oil	4.6 ± 0.7	10–52	Reduced condensates, less secondary reactions
Syngas	64.6 ± 1.6	20–60	Higher gas fraction beneficial for energy recovery

Footnotes: Mass yields (wt.%) of biochar, bio-oil, and syngas obtained under vacuum conditions (this study) are compared with literature ranges for conventional slow pyrolysis at similar temperatures (Aissaoui et al., 2021; Altaf et al., 2025; Tayibi et al., 2021). Results highlight enhanced solid yield and reduced condensable fraction under vacuum operation. Values are mean ± SD (n = 10).

The bio-oil yield was low (4.6 wt.%), consistent with the vacuum process promoting the rapid ejection and gasification of volatiles rather than their condensation into liquid fractions. This shift in product distribution resulted in a high yield of syngas (64.6 wt.%), which is rich in non-condensable gases like CO, CH_4, and H_2. This syngas stream represents a significant energy asset; it can be combusted to provide the process heat required to maintain the pyrolysis temperature and power the vacuum system (Divyangkumar et al., 2024).

3.2. Proximate and ultimate analyses

The proximate analysis revealed substantial compositional changes induced by vacuum pyrolysis (Table 2). The proximate composition of OP showed high VM (79.8%) and moderate FC (5.7%), reflecting its lignocellulosic character with abundance of polysaccharides and lipids. After vacuum pyrolysis, biochar was enriched in carbon (79,8%) and FC (68.7%) while VM decreased to 17.1%. This shift indicates removal of thermally

labile fractions and the enrichment of stable aromatic structures. These values meet benchmarks established by IBI for stable biochar (FC > 60%, VM < 20%), confirming the suitability of the material for long-term carbon storage. In the Tunisian context, Aissaoui et al. (2023) reported a value of 34.8 wt.% for VM and 58.6 wt.% for FC in biochar produced from OP at 500°C using an atmospheric reactor.

Energy performance indicators confirmed the transformation of the material. HHV increased from 14.5 to 27.0 MJ kg^{-1}, corresponding to an energy densification factor of 1.9. The fuel ratio (FC/VM) rose markedly from 0.07 to 4.02, while Ts reached 0.80, reflecting limited mass loss under elevated temperatures. These characteristics indicate that the resulting biochar possesses high calorific quality and could be utilized as an energy-dense solid fuel for thermochemical applications. Comparable improvements in HHV and stability have been reported for lignocellulosic feedstocks subjected to low-pressure pyrolysis conditions (Fakhar et al., 2025; Maaoui et al., 2024).

Table 2. Proximate composition and derived energy indices of olive pomace and its biochar produced by vacuum pyrolysis.

Parameters	Olive pomace	Biochar
Moisture (%)	7.73 ± 0.02	3.01 ± 0.03
VM (%)	79.83 ± 0.82	17.11 ± 0.49
Ash (%)	6.78 ± 0.32	11.16 ± 0.09
Fixed carbon (%)	5.65 ± 0.99	68.72 ± 0.52
HHV (MJ kg^{-1})	14.5	27.0
Energy densification (Ed)	1	1.9
Fuel ratio (Fr)	0.07	4.02
Thermal stability (Ts)	0.07	0.80

Footnotes: Contents are reported as mean ± SD (n = 4). Energy parameters were calculated following Weber and Quicker (2018). All values expressed on a dry-weight basis.

Ash content increased from 6.8% in OP to 11.1% in biochar, indicating concentration of minerals during devolatilization. Furthermore, the concentrated ash fraction is a reservoir of essential plant nutrients like potassium (K), phosphorus (P), and calcium (Ca), which can be slowly released to improve soil fertility (Ippolito et al., 2020).

Elemental analysis confirmed the profound carbonization of olive pomace under vacuum pyrolysis. Carbon content increased markedly from 51.7% in the feedstock to 79.8% in the biochar, accompanied by a sharp reduction in hydrogen (from 6.3% to 0.2%), oxygen (from 40.1% to 18.8%) and slight decrease in nitrogen (from 1.9% to 1.2%). These shifts signify extensive devolatilization and the development of stable carbon framework (McBeath et al., 2014), resulting in very low atomic ratios (H/C = 0.03; O/C = 0.18). This result aligns with previous studies showing that lower atomic ratios (H/C < 0.4 and O/C < 0.2) correspond to condensed aromatic domains highly resistant to microbial degradation. For example, (Aissaoui et al., 2023) reported that olive-pomace biochars produced at 500°C under conventional conditions exhibited H/C = 0.79 and O/C = 0.31, while Tayibi et al. (2021) reported low values (H/C = 0.06 and O/C = 0.17) under same conditions. Such compositional changes confirm that vacuum pyrolysis effectively converts labile biomass into a carbon-rich, mineral-enriched material with high stability potential. As illustrated in the Van Krevelen diagram (Figure 2), the vacuum biochar in this study clearly falls within the IBI and EBC stability zone, confirming its long-term resistance to decomposition and its suitability for carbon sequestration for several centuries (Afshar & Mofatteh, 2024; Rodrigues et al., 2023; Subbiah et al., 2025).

3.3. Rock-Eval pyrolysis

The Rock-Eval results (Figure 3) indicated a marked increase in TOC (42.1% in the raw feedstock to 84.5% in the biochar). This was accompanied by a sharp reduction in the HI (from 561 to 2 mg HC g^{-1} TOC) and OI (from 179 to 17 mg CO_2 g^{-1} TOC), reflecting the extensive loss of aliphatic and oxygenated functional groups (Ahmad et al., 2014; Mishra et al., 2025; Singh et al., 2020). The Tmax shifted from 296 °C in OP to 607 °C in biochar, consistent

with the formation of highly aromatic and thermally stable and recalcitrant carbon phases (Yang et al., 2007).

The very low H/C = 0.03 was independently confirmed by CHNS and Rock-Eval analyses (HI = 2 mg HC g^{-1} TOC), while FTIR spectra (section 3.7) showed the complete disappearance of aliphatic C–H stretching bands in the 2800–3000 cm^{-1} region, indicating extensive dehydrogenation of the carbon matrix. These converging lines of evidence demonstrate that the low hydrogen content reflects a highly condensed aromatic structure. Nevertheless, complementary validation using solid-state ^{13}C NMR would further strengthen this observation. These findings place the produced biochar well within the stability thresholds established by the International Biochar Initiative (HI < 50; Tmax > 600 °C), supporting its long-term persistence in soil environments. This result aligns with previous study (Spokas, 2010) showing that lower atomic ratios correspond to condensed aromatic domains resistant to microbial degradation. Importantly, vacuum conditions limit oxidative losses compared to conventional pyrolysis, yielding a material with both high aromaticity and preserved carbonyl, aromatic, and phenolic functional groups, which are more stable over time (Ahmad et al., 2014).

3.4. Thermogravimetric analysis (TGA/DTG)

Thermogravimetric (TG) and derivative (DTG) curves in Figure 4 provided complementary insights. Olive pomace exhibited three distinct decomposition phases: (i) moisture release and volatilization of light compounds below 150 °C (7% loss), (ii) rapid degradation of hemicellulose and cellulose between 150–400 °C (53% loss), and (iii) gradual decomposition of lignin-derived structures above 400 °C (23% loss). In contrast, the biochar profile showed minimal mass loss, with less than 15% reduction up to 1000°C, confirming the dominance of condensed aromatic structures. The subdued DTG signals further confirmed that most labile

fractions had been eliminated during pyrolysis, leaving only highly recalcitrant carbon domains (Choi et al., 2017). These findings are consistent with the low H/C and O/C ratios, reinforcing the evidence for long-term stability (Spokas et al., 2012; Wu et al., 2025). Taken together, the Rock-Eval and TGA results converge on a single conclusion: vacuum pyrolysis produces a carbon-rich material with high aromaticity and strong resistance to thermal degradation (Keiluweit et al., 2010; Papadopoulou et al., 2023).

3.5. Physicochemical proprieties

The pH rose from 7.8 to 9.8 because of the concentration of basic oxides and carbonates, enhancing its liming value in acidic soils (Murtaza et al., 2024). Electrical conductivity (3.3 ± 0.1 dS m^{-1}) reflected soluble nutrient content but may pose salinity risks to sensitive crops, necessitating site-specific application (Woolf et al., 2021). Low bulk density (0.32 g cm^{-3}) and high porosity (79 %) indicate a lightweight amendment that can improve aeration, water retention, and microbial colonization (Kalu et al., 2024). Coarse particle dominance (>800 µm) limits wind erosion and promotes field persistence. The vacuum-derived biochar exhibited a cation-exchange capacity of 56.2 ± 3.1 cmolc kg^{-1}, exceeding values typical of cereal-straw (15-25) and poultry-litter (25–35) biochars (Ippolito et al., 2020; Yuan et al., 2011). Potassium was the predominant exchangeable cation (46.7 cmolc kg^{-1}), followed by Ca, Na, and Mg, confirming mineral enrichment. Such high CEC indicates strong potential to enhance nutrient-holding capacity in coarse-textured or degraded soils (Chen et al., 2019). Exchangeable P averaged 0.27 cmolc kg^{-1}, implying a complementary rather than substitutive role for P fertilization (Sigua et al., 2016; Yu et al., 2023).

3.6. Mineral composition and nutrient enrichment

Elemental analysis in Figure 5 revealed strong enrichment of biochar, after vacuum pyrolysis, in key agronomic nutrients. Phosphorus concentration increased by nearly 293%, potassium

by 253%, and calcium by 130% compared to the feedstock. Azzaz et al. (2022) reported similar concentration of Ca (1.21 g kg^{-1}) in biochar derived from OP under slow pyrolysis. While K (3.08 g kg-1) and P (0.14 g kg^{-1}) was lower than concentration found in this study, especially for P (0.33 g kg^{-1} in biochar produced under vacuum condition). These findings suggest that conventional pyrolysis results in partial volatilization of nutrients. In contrast, the reduced pressure (15–20 kPa) lowers the evaporation point of organic compounds but does not affect refractory minerals such as $Ca_3(PO_4)_2$. The accumulation of chloride was also observed (+382%), though its level remained within agronomic safety limits. In contrast, minor reductions in Mg, Si, and Fe suggest partial volatilization or redistribution during thermal processing (Albalasmeh et al., 2024; Pellera et al., 2021).

3.7. FTIR spectroscopy

FTIR spectra (Figure 6) provided complementary insights into chemical transformations. In OP, strong bands corresponding to O–H stretching (~3400 cm^{-1}), C–H aliphatic stretching (~2920 cm^{-1}), and C=O stretching (~1720 cm^{-1}) were observed. These signals, matching to polysaccharide and lipid functionalities, diminished after vacuum pyrolysis, replaced by prominent aromatic C=C stretching (~1600 cm^{-1}) and C–O vibrations (~1100 cm^{-1}). The reduction of aliphatic and carbohydrate peaks indicates decomposition of labile fractions, while persistent aromatic peaks confirm enhanced stability and the persistence of oxygenated functionalities that contribute to surface reactivity (Ahmad et al., 2014; Kambo & Dutta, 2015). This agrees with earlier reports where residual hydroxyl and carboxyl groups contribute to cation exchange and nutrient adsorption.

3.8. XRD analysis

XRD patterns of OP (Figure 7) showed poorly ordered carbon structures with peaks attributable to cellulose and mineral phases (calcite, quartz). In vacuum biochar, broad

diffraction around 2θ = 25° indicated the formation of turbostratic carbon layers (graphitic-like domains). Crystalline mineral peaks of calcite and potassium salts were more pronounced, consistent with nutrient enrichment and ash concentration. Peaks corresponding to quartz (26.6°), calcite (29.4°, 39.4°, 47.5°), sylvite (28.3°), and periclase (42.9°) were observed, suggesting that key mineral phases remained stable during pyrolysis (Uras-Postma et al., 2014). These phases may act as slow-release nutrient sources and enhance the biochar's agronomic value.

The partial graphitization is particularly relevant for soil use: while it enhances structural durability, the presence of crystalline mineral inclusions may contribute to pH buffering and nutrient release. These changes were similarly reported for biochar produced through vacuum pyrolysis (Keiluweit et al., 2010; Leng & Huang, 2018).

3.9. SEM observations

SEM micrographs of biochar (Figure 8a) highlighted a porous architecture inherited from the vascular tissues of the feedstock, with preserved cell-wall channels from lignin structures. At higher magnifications (3000×), fine pores and intraparticle mineral deposits were visible (Figure 8b). Such structural features enhance the agronomic value of the biochar by providing sites for microbial colonization, improving water retention, and supporting slow nutrient release. The coexistence of porosity and mineral enrichment suggests a synergistic role in both physical soil conditioning and nutrient supply. These developed structures agree with SEM observations reported by Kavdır et al. (2023) and Zhao et al. (2019). Combined with high CEC and stable aromaticity, these features support the dual role of vacuum biochar as a soil conditioner and a climate-mitigation tool.

3.10. Environmental implications and field potential

The vacuum biochar produced in this study demonstrated a substantial capacity for climate change mitigation. When applying the IPCC methodology and assuming a conservative carbon stabilization efficiency of 70%, the stable sequestered carbon was estimated at 2.05 tCO_2eq per ton of biochar. This 70% value represents a mean stabilization fraction derived from laboratory-controlled environments and adopted by IBI and EBC for biochars produced at intermediate-to-high temperatures (450–600 °C) with H/C < 0.4 and O/C < 0.2, conditions consistent with this study. However, in real field conditions, stabilization can vary widely (from 50% to >85%) depending on feedstock type, pyrolysis atmosphere, and pedoclimatic conditions (Woolf et al., 2021). More accurate estimates would require site-specific modeling incorporating biochar aging kinetics, mineral interactions, and local soil-climate feedbacks". In addition to the sequestered carbon, avoided emissions from energy recovery and reduced residue disposal represent complementary climate benefits, estimated at approximately 0.6 t CO_2 eq t^{-1} biochar. Literature values indicate that natural aerobic and anaerobic degradation of olive mill residues can release 0.4–0.7 tCO_2eq per ton. Nutrient recovery analysis confirmed high retention of K, Ca, and P in crystalline phases. This translates into a fertilizer-equivalent benefit, providing slow-release nutrients while reducing upstream emissions from chemical fertilizer industrial production (3–6 kg CO_2eq kg^{-1} N and 0.8–1.5 kg CO_2eq kg^{-1} P_2O_5 or K_2O). Adding conservative co-benefits of 0.55 tCO_2eq per ton (fertilizer offset and avoided emissions) to stable sequestered carbon (2.05 tCO_2eq per ton), the carbon sequestration potential of OP biochar was estimated at 2.6 tCO_2eq per ton. This value exceeds many agricultural byproducts produced through conventional pyrolysis or composting. It surpasses that reported for date palm biochar (1.53 tCO2eq per ton) produced under vacuum condition (Divyangkumar et al., 2024). While this estimation demonstrates clear climate mitigation potential, its robustness depends on assumptions about field stability,

decomposition dynamics, and system boundaries. Future field-based assessments will be necessary to refine these values and capture indirect effects such as priming of native organic matter or interactions with soil mineral phases (Raj & Jain, 2025).

From an engineering perspective, vacuum pyrolysis offers notable operational advantages. The high syngas fraction (65 wt.%) provides an internal energy source capable of offsetting 70-90 % of the system's thermal demand, reducing external energy inputs. This self-sufficiency, coupled with the elimination of inert gas consumption, lowers operating costs by an estimated 20–25% compared with conventional atmospheric systems (Afshar & Mofatteh, 2024; Subbiah et al., 2025). Scaling toward pilot units would primarily depend on feedstock logistics and vacuum maintenance efficiency, both of which are feasible under current agro-industrial infrastructure in Mediterranean regions. A major limitation of the present work is that the reactor operated only under a single reduced-pressure range (15–20 kPa). The current laboratory setup does not allow safe or stable operation at intermediate or atmospheric pressures, which prevents direct internal comparison across pressure regimes. Consequently, although the performance trends observed here are consistent with literature datasets from conventional atmospheric pyrolysis conducted on similar Tunisian and Mediterranean olive residues, the specific effect of pressure cannot be isolated with full certainty. Future work should include systematic multi-pressure calibration (40 kPa, 60 kPa, or 100 kPa) to quantify pressure-dependent reaction pathways and product distribution.

From an environmental safety perspective, heavy metal concentrations (Table 3) were well below international thresholds, confirming compliance with IBI and EBC standards. While polycyclic aromatic hydrocarbons (PAHs) were not quantified in this study due to analytical constraints, vacuum pyrolysis conditions (rapid volatile evacuation, reduced secondary reactions), are expected to minimize PAH formation compared to atmospheric systems

(Keiluweit et al., 2010; Uras-Postma et al., 2014). Future work will include comprehensive PAH analysis using GC-MS following EPA Method 8270 to ensure compliance with EBC thresholds (<4 mg kg^{-1} for sum of 16 EPA PAHs).

Table 3. Compliance of heavy metals concentrations (n=3) with Maximum Allowed Thresholds for biochar materials set by IBI/EBC.

Heavy metals mg kg^{-1} (dry wt)	Values of this study mg kg^{-1} (dry wt)	Range of Maximum Allowed Thresholds
Cadmium	Not detected	1.4 - 39
Chromium	4.8667 ± 0.3215	93 - 1200
Cobalt	0.1667 ± 0.1155	34 - 100
Copper	32.3 ± 2.6058	143 - 6000
Lead	15.9333 ± 2.2898	121 - 300
Nickel	5.8 ± 0.1	47 - 420
Zinc	44.9 ± 1.562	416 - 7400

From an agronomic standpoint, the nutrient-rich ash fraction of OP-biochar particularly enriched in K (3.5 g kg^{-1}), Ca (1.2 g kg^{-1}), and P (0.33 g kg^{-1}) supports its use as an effective soil conditioner. These mineral constituents originate from thermally stable inorganic salts (KCl, $CaCO_3$, and Ca–P complexes) that persist through pyrolysis and contribute directly to CEC and buffering capacity (Kalu et al., 2024). In addition to supplying slow-release nutrients, OP biochar enhances soil water retention and reduces nutrient leaching, particularly under coarse-textured or degraded Mediterranean soils prone to drought and organic-matter depletion (Woolf et al., 2021). This nutrient efficiency and functional versatility are especially relevant to Mediterranean agroecosystems, where olive cultivation is both intensive and constrained by soil erosion, salinization, and declining organic carbon stocks (Mairech et al., 2021). The high porosity (79%) and basic pH (9.8) of vacuum-derived biochar make it suitable for ameliorating acidic soils and increasing base saturation.

Nevertheless, certain constraints must be acknowledged. The relatively high C/N ratio (68.4) may induce temporary nitrogen immobilization in N-poor soils, while the moderate electrical conductivity (3.3 dS m^{-1}) could present salinity risks for salt-sensitive crops such as beans or citrus (Wang et al., 2022). To optimize agronomic benefits while mitigating potential risks, tailored management strategies are essential: (i) co-composting biochar with manure or plant residues to lower soluble salt concentrations and increase available nitrogen (Shi et al., 2024). (ii) applying conservative doses (2–5 t ha^{-1}) for sensitive crops, while higher rates (up to 10 t ha^{-1}) can be applied for olives and barley in moderately saline soils (Wu et al., 2023). (iii) pre-leaching or washing biochar before application to remove exchangeable salts. (iv) avoiding application in highly saline soils without concurrent gypsum amendment, which can displace Na^+ ions and improve structure. (v) ensuring post-application irrigation to leach excess salts beyond the root zone (Mao et al., 2024).

Adopting such adaptive strategies would ensure that OP biochar functions as a carbon-negative soil amendment, improving fertility, structure, and water dynamics while remaining compatible with the long-term sustainability objectives of Mediterranean agriculture.

4. Conclusion

Vacuum pyrolysis of olive pomace produced a carbon-rich and mineral-enriched biochar meeting international stability and safety criteria.

• Biochar yield: 30.9 ± 1.2 wt.% with 68.7 % fixed carbon.

• Stability indices: H/C = 0.03, O/C = 0.18, Tmax = 607 °C.

• Nutrient enrichment: K (+253 %), P (+293 %), Ca (+130 %) relative to feedstock.

• CEC = 56.2 cmolc kg^{-1} and porosity = 79 %, confirming agronomic potential.

• Carbon sequestration ≈ 2.6 t CO_2 eq t^{-1} biochar.

These results confirm that vacuum pyrolysis improves both carbon retention and nutrient recovery while minimizing process energy demand. Nevertheless, the findings must be interpreted in light of the fact that only one pressure range was investigated. Future multi-pressure experiments will be required to confirm the specific contribution of vacuum conditions. Future work should also quantify organic contaminants, evaluate long-term soil impacts, assess life-cycle performance, and field-scale validation to consolidate its integration into Mediterranean circular-bioeconomy strategies.

CRediT authorship contribution

Walid Chmingui: Conceptualization, Data curation, Formal analysis, Investigation, Methodology, Writing – original draft. **Imene Dridi:** Investigation, Supervision, Validation, Writing – review & editing. **Hanen Zaier:** Data curation, Formal analysis, Resources, Writing – review & editing**. Thomas Z Lerch:** Data curation, Formal analysis, Investigation, Methodology, Resources, Writing – review & editing. **Claude Hammecker:** Investigation, Methodology, Validation, Writing – review & editing**. Mohamed Hachicha:** Conceptualization, Investigation, Methodology, Supervision, Validation, Writing – review & editing.

Acknowledgements

The authors would like to thank LMI-NAILA and IEES-Paris for their support in conducting this research. Acknowledgments are extended to all individuals who were part of this research study, particularly technical staff from INRGREF-Tunis, IO-Tunis, and IEES-Paris.

Declaration of generative AI in scientific writing

During the preparation of this work, the authors acknowledge the use of AI-assisted tools, notably Grammarly, to improve linguistic accuracy, correct grammatical errors, and increase the overall coherence of this article. The authors reviewed and edited the content and take full responsibility for the publication. The use of AI complies with the journal's requirements for transparency and ethical norms in authorship processes.

Data availability

Data will be made available upon reasonable request.

Funding

This research did not receive any specific grant from funding agencies in the public, commercial, or not-for-profit sectors.

Declaration of Competing Interest

The authors declare that they have no known competing financial interests or personal relationships that could have appeared to influence the work reported in this paper.

References

Afshar, M., & Mofatteh, S. (2024). Biochar for a sustainable future: Environmentally friendly production and diverse applications. *Results in Engineering*, *23*. https://doi.org/10.1016/j.rineng.2024.102433

Agbede, T. M., & Oyewumi, A. (2022). Benefits of biochar, poultry manure and biochar–poultry manure for improvement of soil properties and sweet potato productivity in degraded tropical agricultural soils. *Resources, Environment and Sustainability*, *7*. https://doi.org/https://doi.org/10.1016/j.resenv.2022.100051

Ahmad, M., Rajapaksha, A. U., Lim, J. E., Zhang, M., Bolan, N., Mohan, D., Vithanage, M., Lee, S. S., & Ok, Y. S. (2014). Biochar as a sorbent for contaminant management in soil and water: a review. *Chemosphere*, *99*, 19-33. https://doi.org/10.1016/j.chemosphere.2013.10.071

Aissaoui, M. H., Trabelsi, A. B. H., Abidi, S., Zaafouri, K., Haddad, K., Jamaaoui, F., Leahy, J. J., & Kwapinski, W. (2021). Sustainable biofuels and biochar production from olive mill wastes via co-pyrolysis process. *Biomass Conversion and Biorefinery*, *13*(10), 8877-8890. https://doi.org/10.1007/s13399-021-01735-z

Aissaoui, M. H., Trabelsi, A. B. H., bensidhom, G., Ceylan, S., Leahy, J. J., & Kwapinski, W. (2023). Insights into olive pomace pyrolysis conversion to biofuels and biochars: Characterization and techno-economic evaluation. *Sustainable Chemistry and Pharmacy*, *32*. https://doi.org/10.1016/j.scp.2023.101022

Alazzaz, A., Usman, A. R. A., Ahmad, M., Ibrahim, H. M., Elfaki, J., Sallam, A. S., Akanji, M. A., & Al-Wabel, M. I. (2020). Potential short-term negative versus positive effects of olive mill-derived biochar on nutrient availability in a calcareous loamy sand soil. *PLoS One*, *15*(7), e0232811. https://doi.org/10.1371/journal.pone.0232811

Albalasmeh, A. A., Quzaih, M. Z., Gharaibeh, M. A., Rusan, M., Mohawesh, O. E., Rababah, S. R., Alqudah, A., Alghamdi, A. G., & Naserin, A. (2024). Significance of pyrolytic temperature, application rate and incubation period of biochar in improving hydro-physical properties of calcareous sandy loam soil [Article]. *Sci Rep*, *14*(1), 7012, Article 7012. https://doi.org/10.1038/s41598-024-57755-y

Altaf, F., Khan, A., Jahan, Z., & Niazi, M. B. K. (2025). Bioenergy Conversion Strategy of Olive Pomace Using Pyrolysis Process: Effect of Temperature on Yield and Product Analysis. *Arabian Journal for Science and Engineering*, *50*(13), 10023-10038. https://doi.org/10.1007/s13369-025-10022-2

Anvari, S., Aguado, R., Jurado, F., Fendri, M., Zaier, H., Larbi, A., & Vera, D. (2024). Analysis of agricultural waste/byproduct biomass potential for bioenergy: The case of Tunisia. *Energy for Sustainable Development*, *78*. https://doi.org/10.1016/j.esd.2023.101367

ASTM. (2014). ASTM D854-14: Standard Test Methods for Specific Gravity of Soil Solids by Water Pycnometer. https://doi.org/10.1520/D0854-14

ASTM. (2018). ASTM D7481-18: Standard Guide for Microspectrophotometry and Color Measurement in Forensic Paint Analysis. https://doi.org/10.1520/D7481-18

Azzaz, A. A., Matei Ghimbeu, C., Jellai, S., El-Bassi, L., & Jeguirim, M. (2022). Olive Mill by-Products Thermochemical Conversion via Hydrothermal Carbonization and Slow

Pyrolysis: Detailed Comparison between the Generated Hydrochars and Biochars Characteristics. *Processes*, *10*(2). https://doi.org/10.3390/pr10020231

Chaturvedi, S., Singh, S. V., Dhyani, V. C., Govindaraju, K., Vinu, R., & Mandal, S. (2023). Characterization, bioenergy value, and thermal stability of biochars derived from diverse agriculture and forestry lignocellulosic wastes. *Biomass Conversion and Biorefinery*, *13*(2), 879-892. https://doi.org/10.1007/s13399-020-01239-2

Chen, H., Zhang, J., Tang, L., Su, M., Tian, D., Zhang, L., Li, Z., & Hu, S. (2019). Enhanced Pb immobilization via the combination of biochar and phosphate solubilizing bacteria. *Environ Int*, *127*, 395-401. https://doi.org/10.1016/j.envint.2019.03.068

Choi, J., Nam, H., Carter, S., & Capareda, S. C. (2017). Tuning the physicochemical properties of biochar derived from Ashe juniper by vacuum pressure and temperature. *Journal of Environmental Chemical Engineering*, *5*(4), 3649-3655. https://doi.org/10.1016/j.jece.2017.07.028

Divyangkumar, N., Panwar, N. L., Agrawal, C., Gupta, T., Meena, G. L., & Singh, M. (2024). Cradle-to-gate analyses of biochar produced from agricultural crop residues by vacuum pyrolysis. *Clean Energy*, *8*(6), 1-15. https://doi.org/10.1093/ce/zkae069

El-Bassi, L., Azzaz, A. A., Jellali, S., Akrout, H., Marks, E. A. N., Ghimbeu, C. M., & Jeguirim, M. (2021). Application of olive mill waste-based biochars in agriculture: Impact on soil properties, enzymatic activities and tomato growth. *Sci Total Environ*, *755*(Pt 1), 142531. https://doi.org/10.1016/j.scitotenv.2020.142531

Enaime, G., Dababat, S., Wichern, M., & Lubken, M. (2024). Olive mill wastes: from wastes to resources. *Environ Sci Pollut Res Int*, *31*(14), 20853-20880. https://doi.org/10.1007/s11356-024-32468-x

Enebe, M. C., Ray, R. L., & Griffin, R. W. (2025). The impacts of biochar on carbon sequestration, soil processes, and microbial communities: a review. *Biochar*, *7*(1). https://doi.org/10.1007/s42773-025-00499-3

Fakhar, A., Canatoy, R. C., Galgo, S. J. C., Rafique, M., & Sarfraz, R. (2025). Advancements in modified biochar production techniques and soil application: a critical review. *Fuel*, *400*. https://doi.org/10.1016/j.fuel.2025.135745

Goktepeli, G., Ozgan, A., Onen, V., Ahmetli, G., Kalem, M., & Yel, E. (2024). Alternative green application areas for olive pomace catalytic pyrolysis biochar obtained via marble sludge catalyst. *Biodegradation*, *35*(6), 907-938. https://doi.org/10.1007/s10532-024-10088-z

Hossain, M. Z., Bahar, M. M., Sarkar, B., Donne, S. W., Ok, Y. S., Palansooriya, K. N., Kirkham, M. B., Chowdhury, S., & Bolan, N. (2020). Biochar and its importance on nutrient dynamics in soil and plant. *Biochar*, *2*(4), 379-420. https://doi.org/10.1007/s42773-020-00065-z

İlay, R. (2020). Short-lived Effects of Olive Pomace Biochar Produced at Different Temperatures on Nitrate (NO3-), Bromide (Br-), Sulfate (SO42-) and Phosphate (PO43-) Leaching from Sandy Loam Soils. *Communications in Soil Science and Plant Analysis*, *51*(17), 2223-2243. https://doi.org/10.1080/00103624.2020.1822375

IPCC, I. P. o. C. C. (2019). *2019 Refinement to the 2006 IPCC Guidelines for National Greenhouse Gas Inventories – Volume 4: Agriculture, Forestry and Other Land Use (AFOLU)*. https://www.ipcc-nggip.iges.or.jp/public/2019rf/index.html

Ippolito, J. A., Cui, L. Q., Kammann, C., Wrage-Mönnig, N., Estavillo, J. M., Fuertes-Mendizabal, T., Cayuela, M. L., Sigua, G., Novak, J., Spokas, K., & Borchard, N. (2020). Feedstock choice, pyrolysis temperature and type influence biochar characteristics: a comprehensive meta-data analysis review. *Biochar*, *2*(4), 421-438. https://doi.org/10.1007/s42773-020-00067-x

Kalu, S., Seppänen, A., Mganga, K. Z., Sietiö, O. M., Glaser, B., & Karhu, K. (2024). Biochar reduced the mineralization of native and added soil organic carbon: evidence of negative priming and enhanced microbial carbon use efficiency. *Biochar*, *6*(1). https://doi.org/https://doi.org/10.1007/s42773-023-00294-y

Kambo, H. S., & Dutta, A. (2015). A comparative review of biochar and hydrochar in terms of production, physico-chemical properties and applications. *Renewable & Sustainable Energy Reviews*, *45*, 359-378. https://doi.org/10.1016/j.rser.2015.01.050

Kavdır, Y., İlay, R., Güven, O. B., & Sungur, A. (2023). Characterization of olive pomace biochar produced at different temperatures and their temporal effects on soil aggregation and carbon content. *Biomass Conversion and Biorefinery*, *14*(16), 19305-19314. https://doi.org/10.1007/s13399-023-03900-y

Keiluweit, M., Nico, P. S., Johnson, M. G., & Kleber, M. (2010). Dynamic molecular structure of plant biomass-derived black carbon (biochar) [Article]. *Environ Sci Technol*, *44*(4), 1247-1253. https://doi.org/10.1021/es9031419

Leng, L., & Huang, H. (2018). An overview of the effect of pyrolysis process parameters on biochar stability [Review]. *Bioresour Technol*, *270*, 627-642. https://doi.org/10.1016/j.biortech.2018.09.030

Lustosa Filho, J. F., da Silva, A. P. F., Costa, S. T., Gomes, H. T., de Figueiredo, T., & Hernández, Z. (2024). Biochars Derived from Olive Mill Byproducts: Typology, Characterization, and Eco-Efficient Application in Agriculture—A Systematic Review [Review]. *Sustainability*, *16*(12), Article 5004. https://doi.org/10.3390/su16125004

Maaoui, A., Chagtmi, R., Lopez, G., Cortazar, M., Olazar, M., & Trabelsi, A. B. H. (2024). Impact of pyrolysis process conditions on the features of the biochar from Opuntia ficus indica fruit peels. *Biomass Conversion and Biorefinery*, *15*(6), 8771-8791. https://doi.org/10.1007/s13399-024-05750-8

Mairech, H., López-Bernal, Á., Moriondo, M., Dibari, C., Regni, L., Proietti, P., Villalobos, F. J., & Testi, L. (2021). Sustainability of olive growing in the Mediterranean area under future climate scenarios: Exploring the effects of intensification and deficit irrigation. *European Journal of Agronomy*, *129*. https://doi.org/10.1016/j.eja.2021.126319

Mao, T., Wang, Y., Ning, S., Mao, J., Sheng, J., & Jiang, P. (2024). Assessment of the Effects of Biochar on the Physicochemical Properties of Saline–Alkali Soil Based on Meta-Analysis. *Agronomy*, *14*(10). https://doi.org/10.3390/agronomy14102431

Marks, E. A. N., Kinigopoulou, V., Akrout, H., Azzaz, A. A., Doulgeris, C., Jellali, S., Rad, C., Zulueta, P. S., Tziritis, E., El-Bassi, L., Ghimbeu, C. M., & Jeguirim, M. (2020). Potential for Production of Biochar-Based Fertilizers from Olive Mill Waste in Mediterranean Basin Countries: An Initial Assessment for Spain, Tunisia, and Greece. *Sustainability*, *12*(15). https://doi.org/https://doi.org/10.3390/su12156081

Martínez-Toledo, C., Valdes-Vidal, G., Calabi-Floody, A., González, M. E., Ruiz, A., Mignolet-Garrido, C., & Norambuena-Contreras, J. (2025). Optimising slow pyrolysis parameters to enhance biochar European hazelnut shell as a biobased asphalt modifier. *Materials Today Sustainability*, *30*. https://doi.org/10.1016/j.mtsust.2025.101087

McBeath, A. V., Smernik, R. J., Krull, E. S., & Lehmann, J. (2014). The influence of feedstock and production temperature on biochar carbon chemistry: A solid-state 13C NMR study. *Biomass and Bioenergy*, *60*, 121-129. https://doi.org/10.1016/j.biombioe.2013.11.002

Miranda, T., Esteban, A., Rojas, S., Montero, I., & Ruiz, A. (2008). Combustion analysis of different olive residues. *Int J Mol Sci*, *9*(4), 512-525. https://doi.org/10.3390/ijms9040512

Mishra, R. K., Chinnam, S., & Sharma, A. (2025). Thermocatalytic pyrolysis of low-value waste biomass: Thermal decomposition, kinetics behaviour, and biochar characterization. *Results in Engineering*, *25*. https://doi.org/10.1016/j.rineng.2025.104210

Munzeiwa, W. A., Tsekoa, P., Kammies, L. R. D., Chelechele, K., Oluwalana-Sanusi, A. E., & Chaukura, N. (2025). Influence of biomass baseline potential on biochar properties and performance for targeted applications. *Discover Water*, *5*(1). https://doi.org/10.1007/s43832-025-00254-6

Murtaza, G., Usman, M., Iqbal, J., Hyder, S., Solangi, F., Iqbal, R., Okla, M. K., Al-Ghamdi, A. A., Elsalahy, H. H., Tariq, W., & Al-Elwany, O. (2024). Liming potential and characteristics of biochar produced from woody and non-woody biomass at different pyrolysis temperatures. *Sci Rep*, *14*(1), 11469. https://doi.org/10.1038/s41598-024-61974-8

P. Rueda, M., Comino, F., Aranda, V., Domínguez-Vidal, A., & Ayora-Cañada, M. J. (2022). Analytical pyrolysis (Py-GC-MS) for the assessment of olive mill pomace composting efficiency and the effects of compost thermal treatment. *Journal of Analytical and Applied Pyrolysis*, *168*. https://doi.org/10.1016/j.jaap.2022.105711

Papadopoulou, K., Tarani, E., Ainali, N. M., Chrissafis, K., Wurzer, C., Masek, O., & Bikiaris, D. N. (2023). The Effect of Biochar Addition on Thermal Stability and Decomposition Mechanism of Poly(butylene succinate) Bionanocomposites. *Molecules*, *28*(14). https://doi.org/10.3390/molecules28145330

Pellera, F. M., Regkouzas, P., Manolikaki, I., & Diamadopoulos, E. (2021). Biochar Production from Waste Biomass: Characterization and Evaluation for Agronomic and Environmental Applications [Article]. *Detritus*, *17*, 15-29. https://doi.org/10.31025/2611-4135/2021.15146

Raj, R. S., & Jain, S. (2025). Assessment of Municipal Solid Waste Torrefaction for Sustainable Biochar Production: A Comprehensive Life Cycle Evaluation of Eight Process Scenarios. *Results in Engineering*. https://doi.org/10.1016/j.rineng.2025.107025

Rambhatla, N., Panicker, T. F., Mishra, R. K., Manjeshwar, S. K., & Sharma, A. (2025). Biomass pyrolysis for biochar production: Study of kinetics parameters and effect of temperature on biochar yield and its physicochemical properties. *Results in Engineering*, *25*. https://doi.org/10.1016/j.rineng.2024.103679

Ravindiran, G., Rajamanickam, S., Janardhan, G., Hayder, G., Alagumalai, A., Mahian, O., Lam, S. S., & Sonne, C. (2024). Production and modifications of biochar to engineered materials and its application for environmental sustainability: a review. *Biochar*, *6*(1). https://doi.org/10.1007/s42773-024-00350-1

Rodrigues, L., Budai, A., Elsgaard, L., Hardy, B., Keel, S. G., Mondini, C., Plaza, C., & Leifeld, J. (2023). The importance of biochar quality and pyrolysis yield for soil carbon sequestration in practice. *European Journal of Soil Science*, *74*(4). https://doi.org/10.1111/ejss.13396

Roy, C., Chaala, A., Darmstadt, H., De Caumia, B., Pakdel, H., & Yang, J. (2005). Conversion of used tires to carbon black and oil by pyrolysis. In *Rubber Recycling* (pp. 429-468). CRC Press.

Ruan, J. J., Huang, J. X., Qin, B. J., & Dong, L. P. (2018). Heat Transfer in Vacuum Pyrolysis of Decomposing Hazardous Plastic Wastes. *ACS Sustainable Chemistry & Engineering*, *6*(4), 5424-5430. https://doi.org/10.1021/acssuschemeng.8b00255

Sharma, T., Hakeem, I. G., Gupta, A. B., Joshi, J., Shah, K. L., Vuppaladadiyam, A. K., & Sharma, A. (2024). Parametric influence of process conditions on thermochemical

techniques for biochar production: A state-of-the-art review. *Journal of the Energy Institute*, *113*. https://doi.org/10.1016/j.joei.2024.101559

Shi, G., Li, H., Fu, Q., Li, T., Hou, R., Chen, Q., & Xue, P. (2024). Effects of biochar and compost on the abundant and rare microbial communities assembly and multifunctionality in pesticide-contaminated soil under freeze–thaw cycles. *Environ Pollut*, *362*, 125003. https://doi.org/10.1016/j.envpol.2024.125003

Sigua, G. C., Novak, J. M., Watts, D. W., Johnson, M. G., & Spokas, K. (2016). Efficacies of designer biochars in improving biomass and nutrient uptake of winter wheat grown in a hard setting subsoil layer. *Chemosphere*, *142*, 176-183. https://doi.org/10.1016/j.chemosphere.2015.06.015

Singh, R. K., Chakraborty, J. P., & Sarkar, A. (2020). Optimizing the torrefaction of pigeon pea stalk (cajanus cajan) using response surface methodology (RSM) and characterization of solid, liquid and gaseous products. *Renewable Energy*, *155*, 677-690. https://doi.org/10.1016/j.renene.2020.03.184

Spokas, K. A. (2010). Review of the stability of biochar in soils: predictability of O:C molar ratios. *Carbon Management*, *1*(2), 289-303. https://doi.org/10.4155/Cmt.10.32

Spokas, K. A., Cantrell, K. B., Novak, J. M., Archer, D. W., Ippolito, J. A., Collins, H. P., Boateng, A. A., Lima, I. M., Lamb, M. C., McAloon, A. J., Lentz, R. D., & Nichols, K. A. (2012). Biochar: a synthesis of its agronomic impact beyond carbon sequestration. *J Environ Qual*, *41*(4), 973-989. https://doi.org/10.2134/jeq2011.0069

Subbiah, G., Singh, R. P., Deepak, K., Nayak, P. P., venkadeshwaran, K., Tiwari, A., Sahoo, J., & Priya K, K. (2025). Continuous Pyrolysis of Rice Husk for Sustainable Biochar Production and Carbon Sequestration: Recent Advances and Techno-Economic Perspectives. *Results in Engineering*. https://doi.org/10.1016/j.rineng.2025.106991

Tayibi, S., Monlau, F., Fayoud, N. E., Abdeljaoued, E., Hannache, H., Zeroual, Y., Oukarroum, A., & Barakat, A. (2021). Production and Dry Mechanochemical Activation of Biochars Derived from Moroccan Red Macroalgae Residue and Olive Pomace Biomass for Treating Wastewater: Thermodynamic, Isotherm, and Kinetic Studies. *ACS Omega*, *6*(1), 159-171. https://doi.org/10.1021/acsomega.0c04020

Uras-Postma, U., Carrier, M., & Knoetze, J. (2014). Vacuum pyrolysis of agricultural wastes and adsorptive criteria description of biochars governed by the presence of oxides. *Journal of Analytical and Applied Pyrolysis*, *107*, 123-132. https://doi.org/10.1016/j.jaap.2014.02.012

Vandana, T. U., Tripathy, B. K., Mishra, R. K., Sharma, A., & Mohanty, K. (2025). A review on waste biomass-derived biochar: Production, characterisation, and advanced analytical techniques for pollutants assessment in water and wastewater. *Process Safety and Environmental Protection*, *201*. https://doi.org/10.1016/j.psep.2025.107505

Vilas-Boas, A. C. M., Tarelho, L. A. C., Oliveira, H. S. M., Silva, F. G. C. S., Pio, D. T., & Matos, M. A. A. (2024). Valorisation of residual biomass by pyrolysis: influence of process conditions on products. *Sustainable Energy & Fuels*, *8*(2), 379-396. https://doi.org/10.1039/d3se01216f

Wang, Z., Wang, H., Zhao, C., Yang, K., Li, Z., & Yin, K. (2022). Effects of Biochar on the Microenvironment of Saline-Sodic Soil and Maize Growth. *Agronomy*, *12*(11). https://doi.org/10.3390/agronomy12112859

Weber, K., & Quicker, P. (2018). Properties of biochar [Review]. *Fuel*, *217*, 240-261. https://doi.org/10.1016/j.fuel.2017.12.054

Woolf, D., Lehmann, J., Ogle, S., Kishimoto-Mo, A. W., McConkey, B., & Baldock, J. (2021). Greenhouse Gas Inventory Model for Biochar Additions to Soil. *Environ Sci Technol*, *55*(21), 14795-14805. https://doi.org/10.1021/acs.est.1c02425

Wu, Y., Wang, X., Zhang, L., Zheng, Y., Liu, X., & Zhang, Y. (2023). The critical role of biochar to mitigate the adverse impacts of drought and salinity stress in plants. *Front Plant Sci*, *14*, 1163451. https://doi.org/10.3389/fpls.2023.1163451

Wu, Z. Q., Fan, Y. Q., Zhou, Z. Q., Hao, X. M., & Kang, S. Z. (2025). Interaction between biochar particle size and soil salinity levels on soil properties and tomato yield. *Biochar*, *7*(1). https://doi.org/10.1007/s42773-024-00417-z

Yaashikaa, P. R., Kumar, P. S., Varjani, S., & Saravanan, A. (2020). A critical review on the biochar production techniques, characterization, stability and applications for circular bioeconomy. *Biotechnol Rep (Amst)*, *28*, e00570. https://doi.org/10.1016/j.btre.2020.e00570

Yang, H. P., Yan, R., Chen, H. P., Lee, D. H., & Zheng, C. G. (2007). Characteristics of hemicellulose, cellulose and lignin pyrolysis. *Fuel*, *86*(12-13), 1781-1788. https://doi.org/10.1016/j.fuel.2006.12.013

Yu, L., Caldararu, S., Ahrens, B., Wutzler, T., Schrumpf, M., Helfenstein, J., Pistocchi, C., & Zaehle, S. (2023). Improved representation of phosphorus exchange on soil mineral surfaces reduces estimates of phosphorus limitation in temperate forest ecosystems. *Biogeosciences*, *20*(1), 57-73. https://doi.org/10.5194/bg-20-57-2023

Yuan, J. H., Xu, R. K., & Zhang, H. (2011). The forms of alkalis in the biochar produced from crop residues at different temperatures. *Bioresour Technol*, *102*(3), 3488-3497. https://doi.org/10.1016/j.biortech.2010.11.018

Zhao, C. Y., Shi, Y., Xie, J. J., Lei, F., & Zhang, L. (2019). Direct measurement of electrical conductivity of porous biochar monolith for supercapacitors. *Materials Research Express*, *6*(9). https://doi.org/10.1088/2053-1591/ab326e

Figure captions

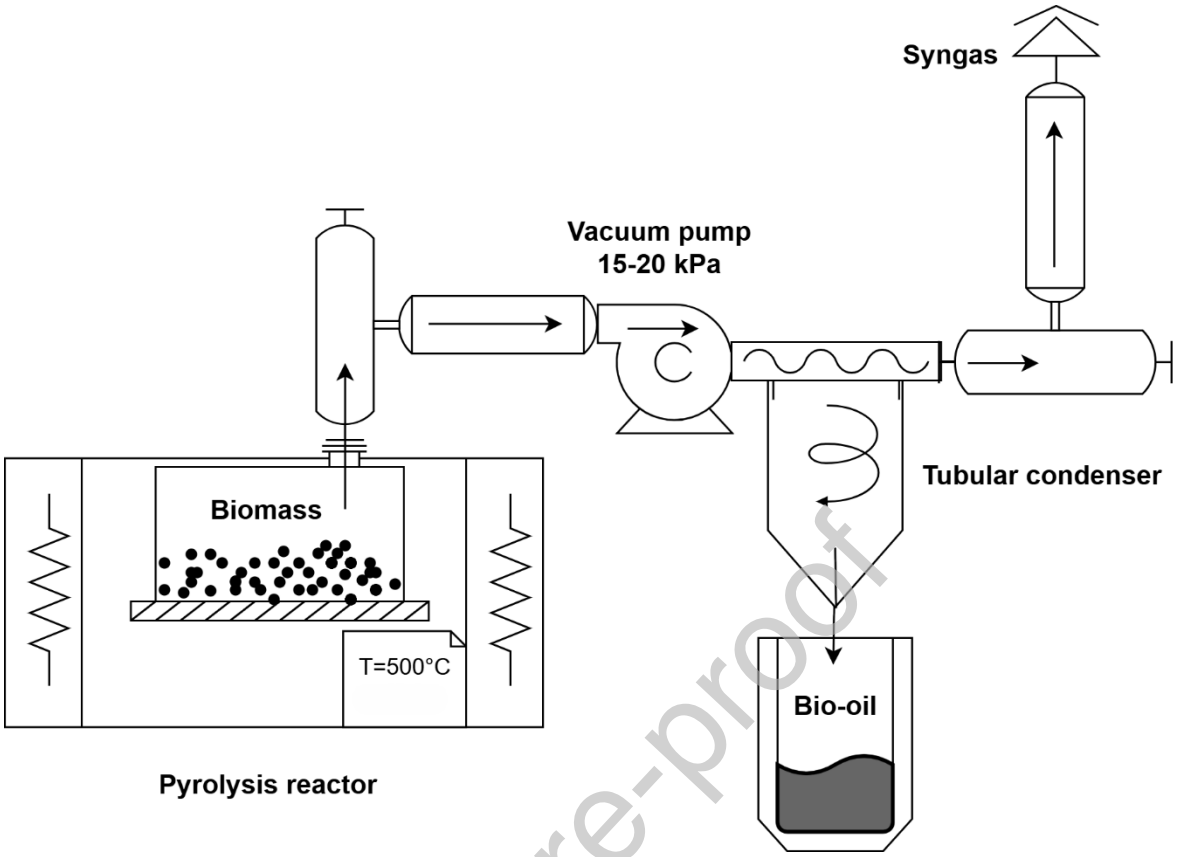

Figure 1. Schematic diagram of the laboratory-scale vacuum pyrolysis system. The setup comprises a muffle furnace, sealed stainless-steel reactor, vacuum pump (15–20 kPa), condensation train for bio-oil recovery, and gas-collection cylinder. Arrows indicate volatile flow and heat transfer. The configuration maintains oxygen-free conditions and ensures reproducible thermal control for olive-pomace conversion at 500 °C.

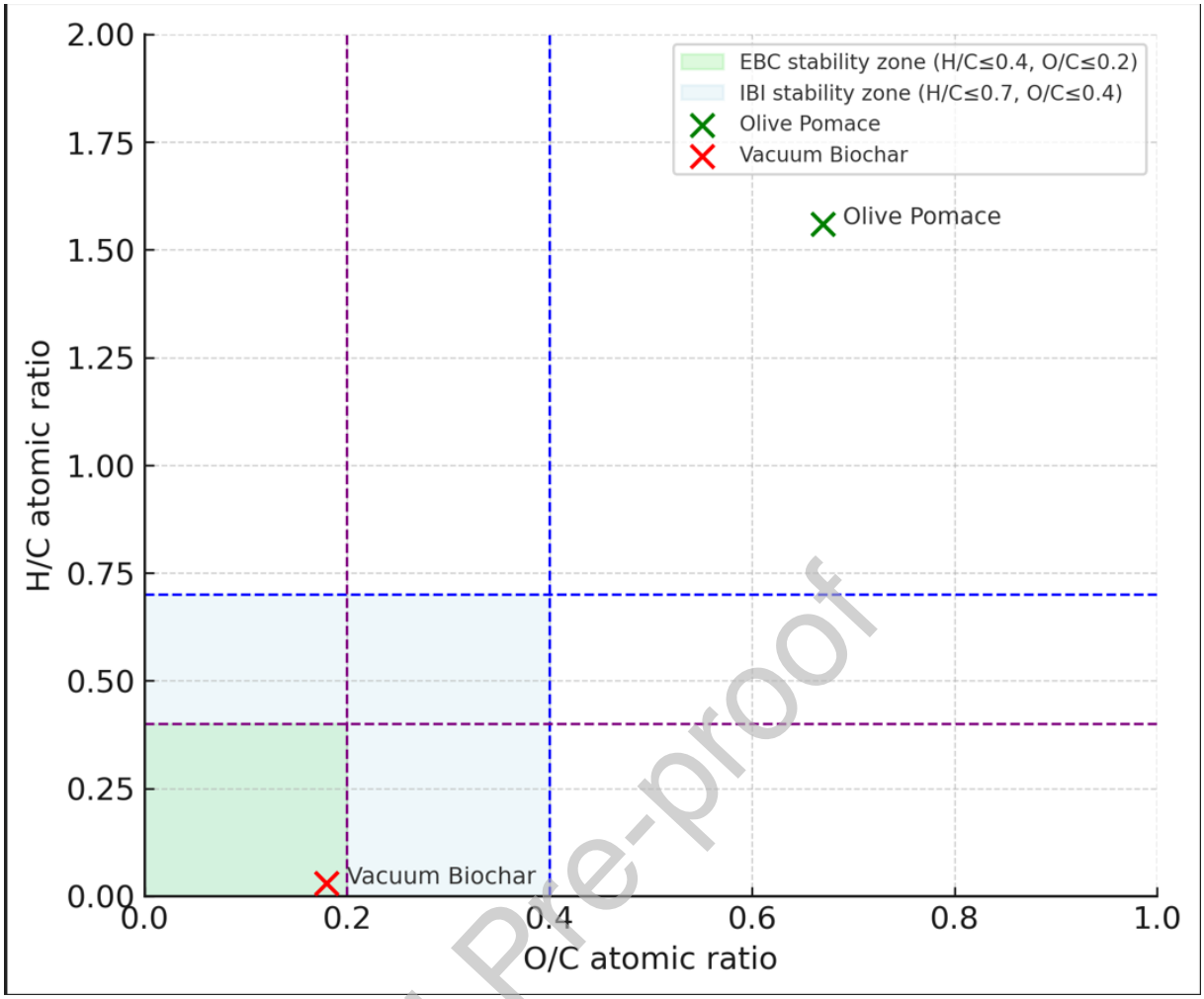

Figure 2. Van Krevelen diagram illustrating elemental transformations during vacuum pyrolysis of olive pomace. Points represent atomic H/C and O/C ratios of feedstock and biochar. The pronounced shift toward lower ratios (H/C = 0.03; O/C = 0.18) indicates extensive dehydrogenation, aromatization, and long-term carbon stability within IBI/EBC certification domains.

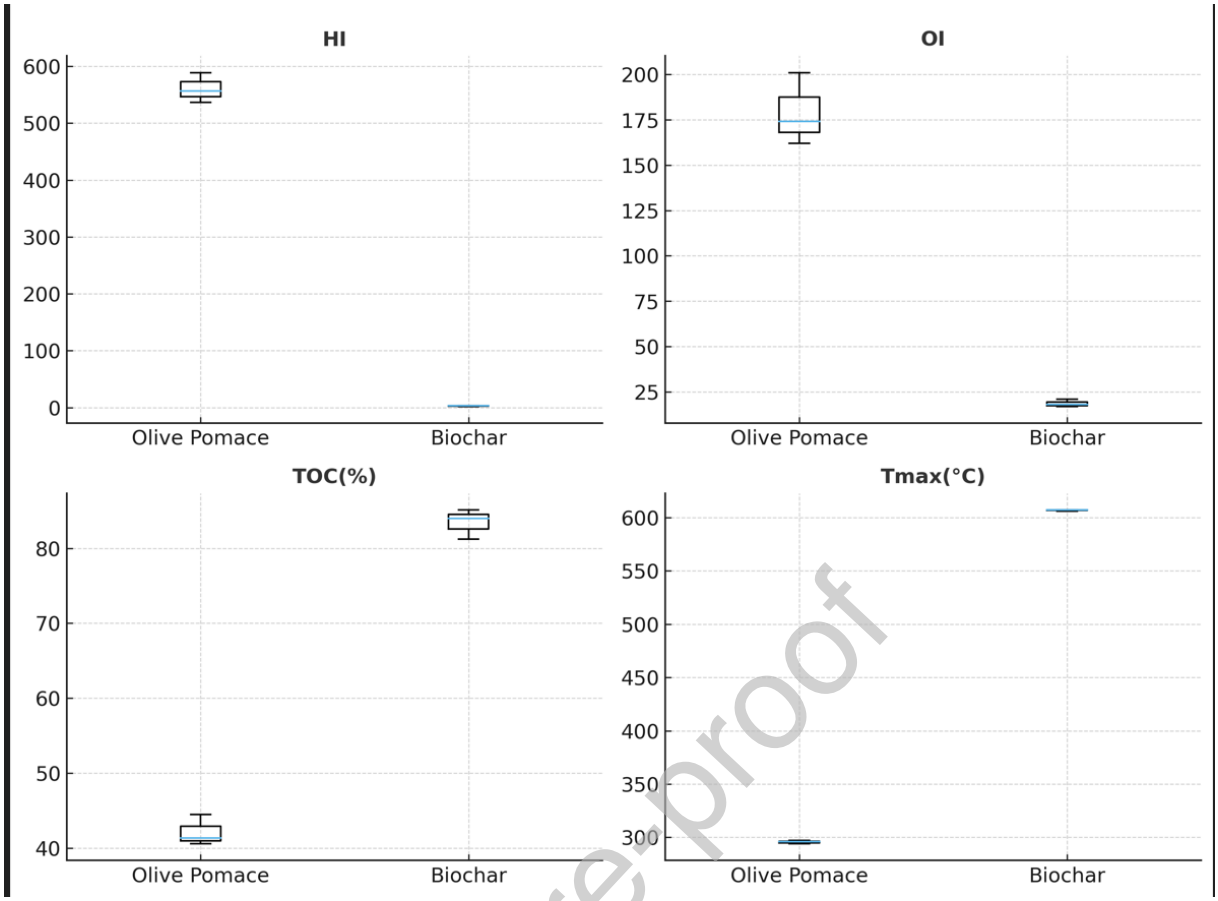

Figure 3. Rock-Eval indices (HI, OI, Tmax, TOC) of olive pomace and vacuum-pyrolyzed biochar. Indices are plotted as mean ± SD (n=4). The sharp decrease in HI and OI, together with a shift in Tmax to higher values, confirms the transformation of labile organic matter into stable, aromatic carbon domains. TOC enrichment reflects enhanced carbon sequestration potential.

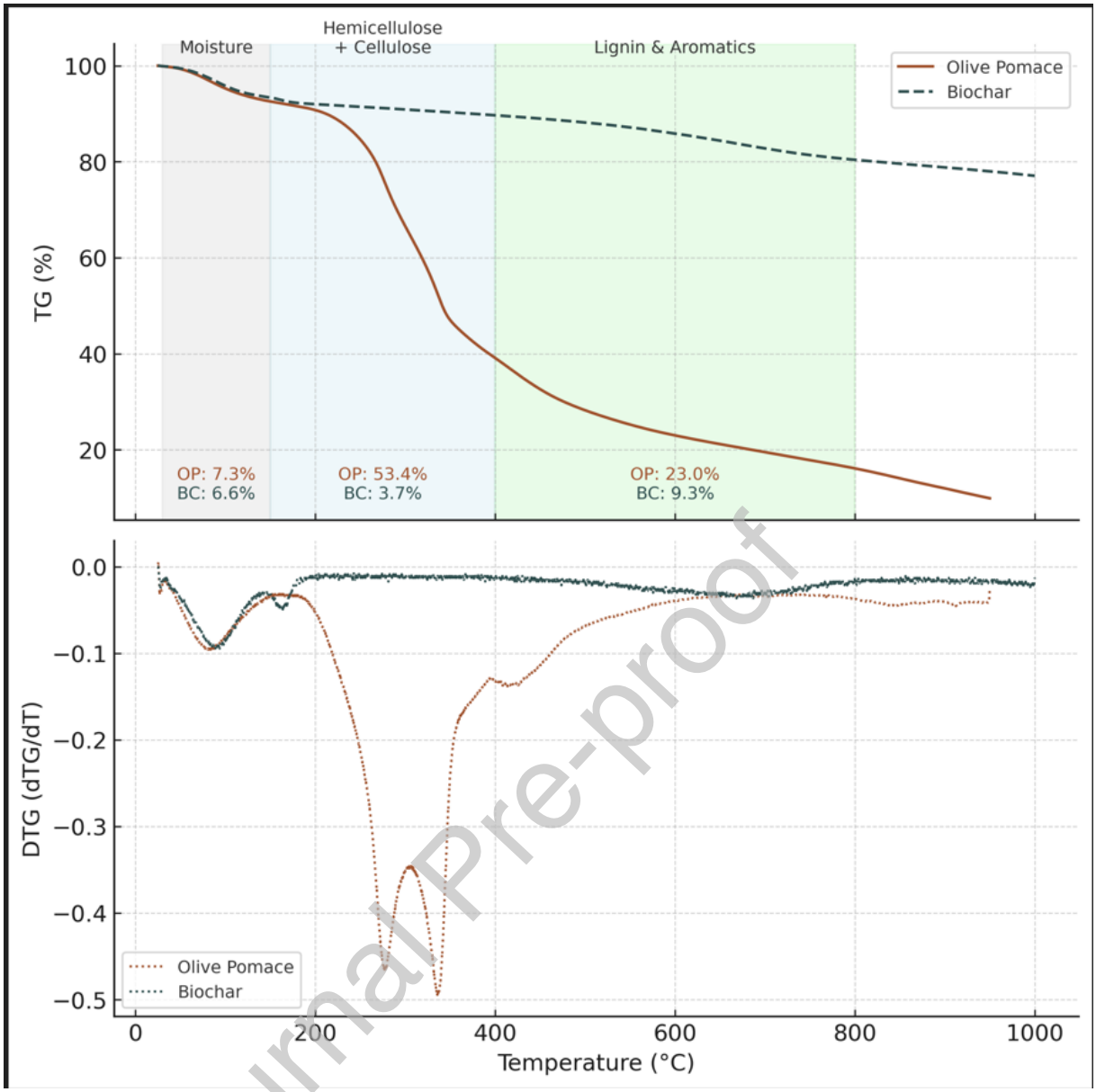

Figure 4. Thermogravimetric (TG) and derivative (DTG) curves of olive pomace and produced biochar. (n=3) Mass-loss profiles show three degradation stages in the feedstock (moisture release < 150 °C, hemicellulose/cellulose decomposition 150–400 °C, lignin breakdown > 400 °C). Biochar exhibits minimal mass loss (< 15 %) up to 1000 °C, confirming formation of condensed, thermally stable carbon structures.

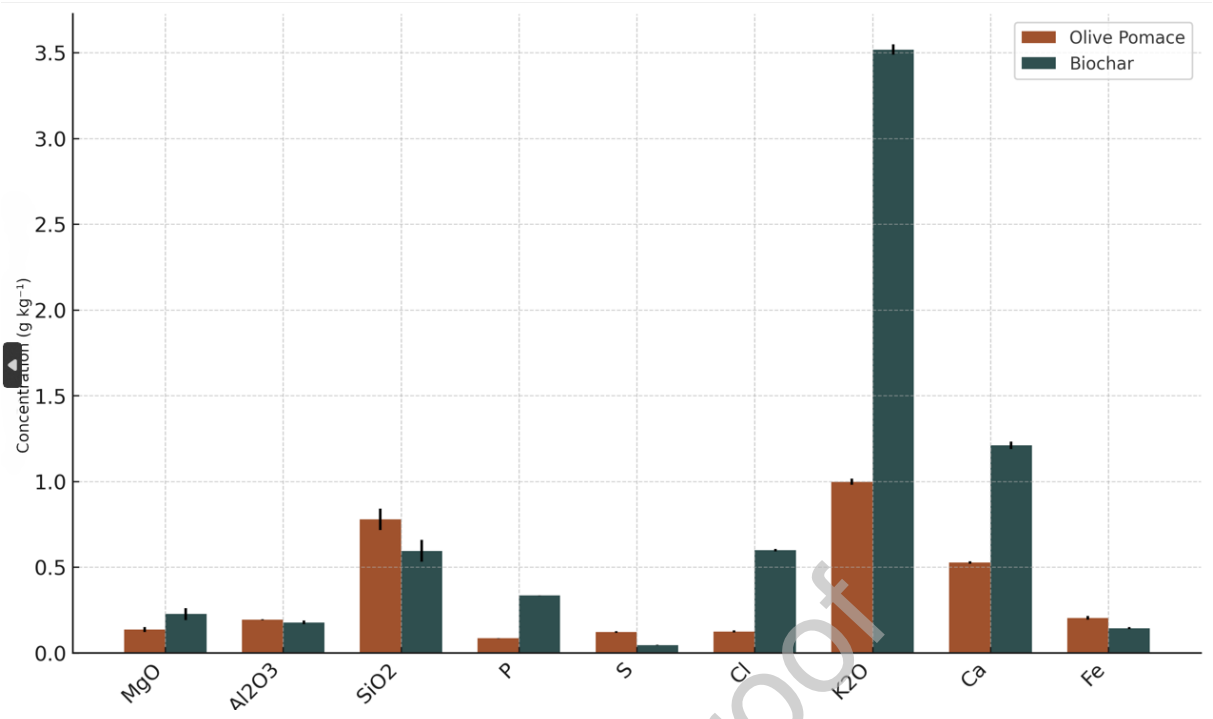

Figure 5. Mineral composition of olive-pomace feedstock and resulting biochar. Bar plots compare concentrations of major nutrients and trace elements determined by ICP-OES. Significant enrichment in K, P, and Ca was observed after vacuum pyrolysis, while Mg and Fe showed slight decreases. Error bars denote ± SD (n = 3).

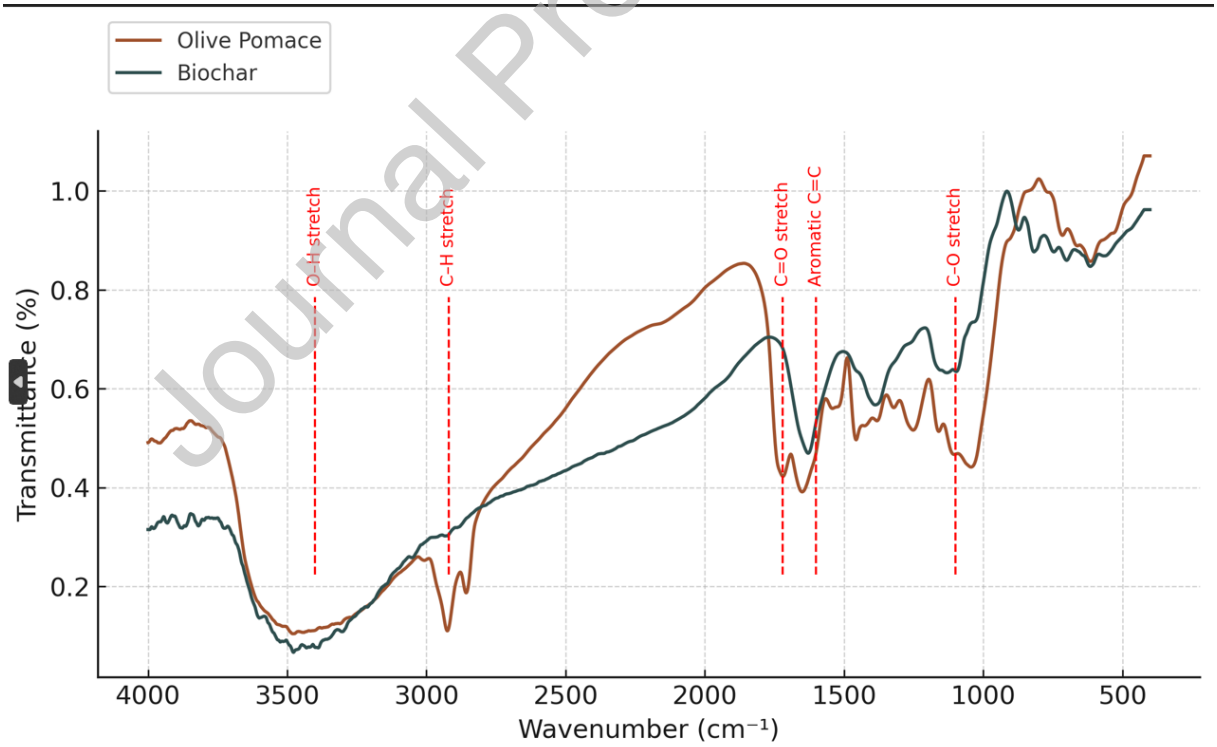

Figure 6. FTIR spectra of olive pomace and vacuum-pyrolyzed biochar. Spectra (4000–400 cm^{-1}) display disappearance of O–H, aliphatic C–H, and carbonyl C=O bands and emergence of aromatic C=C and C–O vibrations, indicating decomposition of labile components and development of aromatic, oxygenated surfaces conducive to cation exchange.

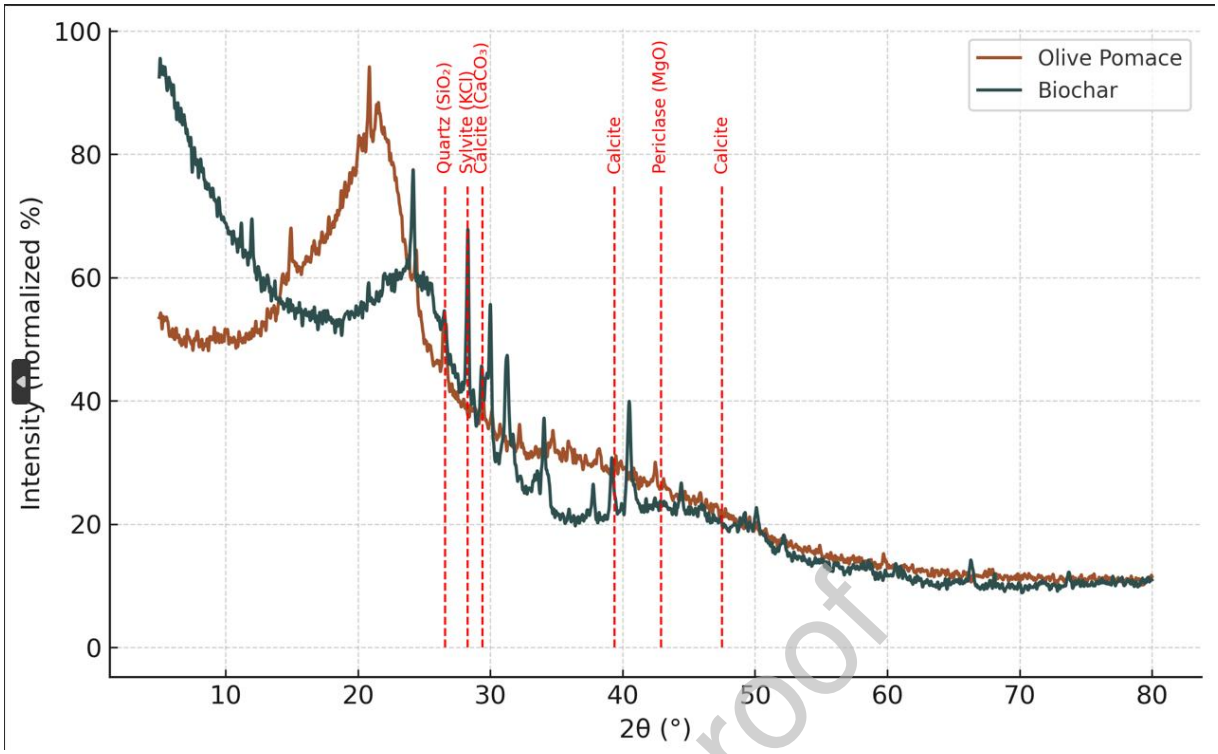

Figure 7. X-ray diffraction (XRD) patterns of olive pomace and derived biochar. Broad peaks near $2\theta \approx 25°$ denote turbostratic carbon layers (incipient graphitization). Distinct reflections for calcite, quartz, sylvite, and periclase confirm preservation of crystalline mineral phases contributing to pH buffering and nutrient release.

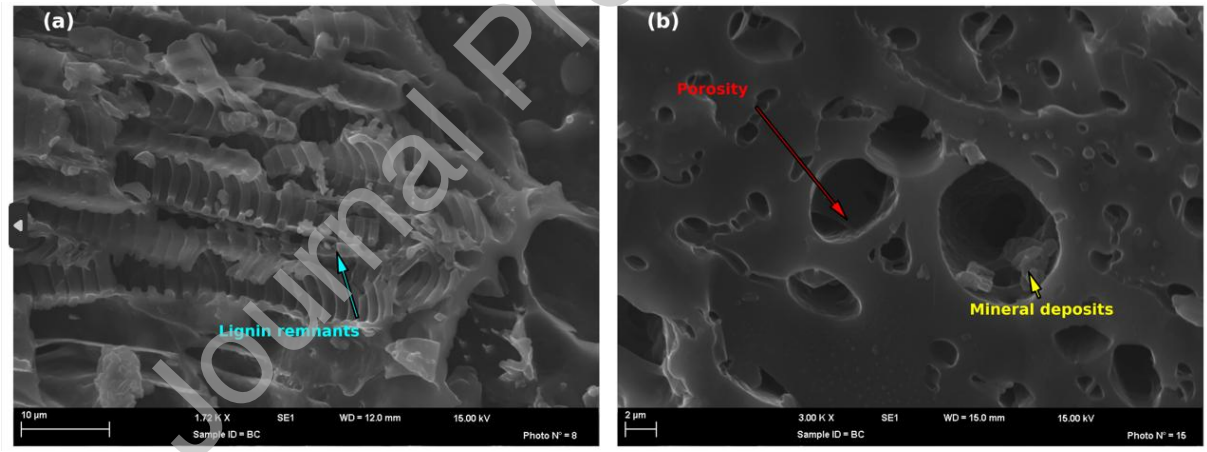

Figure 8. Scanning electron micrographs of vacuum-pyrolyzed biochar. (a) Low-magnification view (1720×) showing preserved vascular channels and macroporosity inherited from the feedstock. (b) High-magnification view (3000×) revealing micropores and mineral deposits rich in Ca and K. The hierarchical pore network enhances water retention, microbial colonization, and nutrient adsorption capacity.

Graphical abstract

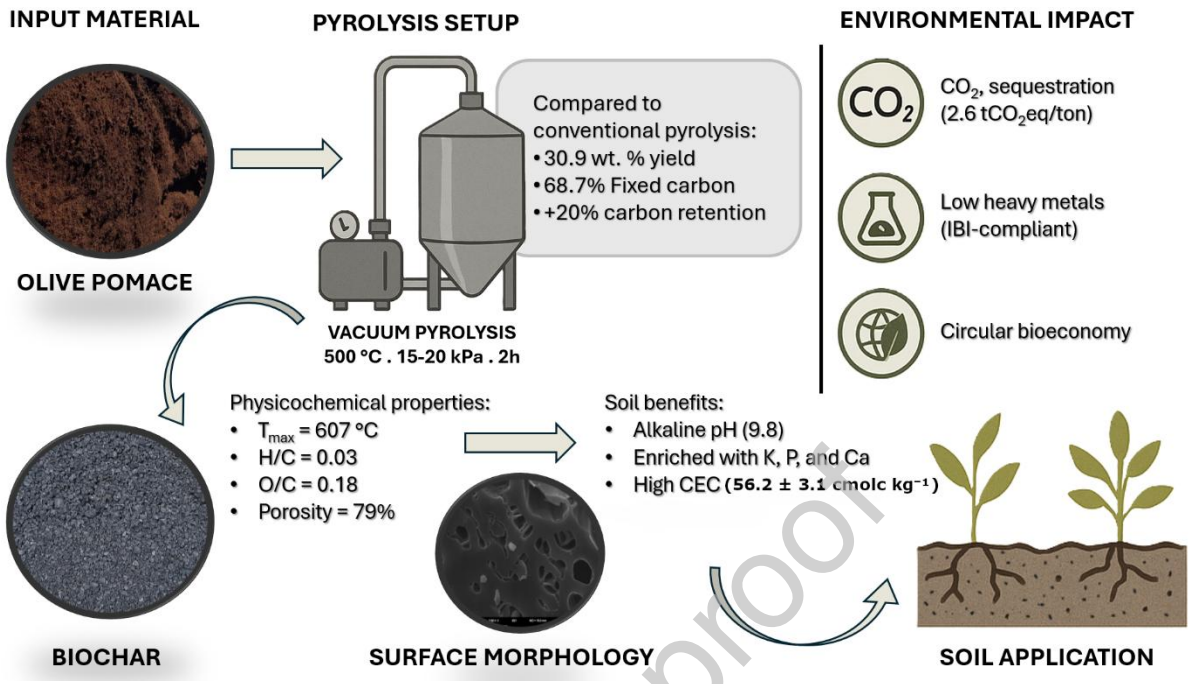

Declaration of interests

☒ The authors declare that they have no known competing financial interests or personal relationships that could have appeared to influence the work reported in this paper.

☐ The authors declare the following financial interests/personal relationships which may be considered as potential competing interests: